Calcif Tissue Int (2017) 100:641–652
DOI 10.1007/s00223-017-0249-4

ORIGINAL RESEARCH

Effect of SDF-1/Cxcr4 Signaling Antagonist AMD3100 on Bone Mineralization in Distraction Osteogenesis

Jia Xu[1] · Yuanfeng Chen[2,3] · Yang Liu[2] · Jinfang Zhang[2] · Qinglin Kang[1] · Kiwai Ho[2] · Yimin Chai[1] · Gang Li[2]

Received: 28 December 2016 / Accepted: 30 January 2017 / Published online: 16 March 2017

Abstract Distraction osteogenesis (DO) is a widely applied technique in orthopedics surgery, which involves rapid stem cell migration, homing, and differentiation. Interactions between the chemokine receptor Cxcr4 and its ligand, stromal derived factor-1 (SDF-1), regulate hematopoietic stem cell trafficking to the ischemic area and induce their subsequent differentiation. Here, we examined SDF-1 expression and further investigated the role of SDF-1/Cxcr4 signaling antagonist AMD3100 during bone regeneration in rat DO model. The results showed that expression levels of SDF-1 and osteogenic genes were higher in DO zones than in the fracture zones, and SDF-1 expression level was the highest at the termination of the distraction phase. Radiological, mechanical, and histological analyses demonstrated that the local administration of AMD3100 (400 μM) to DO rats significantly inhibited new bone formation. In the rat bone marrow mesenchymal stem cells culture, comparing to the group treated with osteogenic induction medium, AMD3100 supplement led to a considerable decrease in the expression of alkaline phosphatase and early osteogenic marker genes. However, the amount of calcium deposits in rat MSCs did not differ between the groups. Therefore, our study demonstrated that the DO process induced higher expression of SDF-1, which collated to rapid induction of callus formation. Local application of SDF-1/Cxcr4 signaling antagonist AMD3100 significantly inhibited bone mineralization and osteogenesis in DO, which may represent a potential therapeutic approach to the enhancement of bone consolidation in patients undergoing DO.

Keywords Stromal cell-derived factor-1 · AMD3100 · Distraction osteogenesis · Bone regeneration · Fracture

Introduction

Distraction osteogenesis (DO) is a technique applied in orthopedic surgery for the reconstruction of skeletal deformities and bone defects [1, 2]. Living tissues can become metabolically activated when subjected to slow and steady traction (strain force), which is characterized by the stimulation of proliferative and biosynthetic cellular functions [3]. Despite the successful induction of tissue regeneration in DO, the clinical protocols are still hampered by the lengthy consolidation period [4]. Recent investigations indicated that the molecular signaling cascade plays a vital role in the process of mechanical strain-induced tissue regeneration [2]. Therefore, the understanding of the molecular mechanisms underlying this process would help enhance callus formation and reduce long DO consolidation period.

Jia Xu and Yuanfeng Chen contributed equally as first authors.

✉ Yimin Chai
ymchai@sjtu.edu.cn

✉ Gang Li
gangli@cuhk.edu.hk

[1] Department of Orthopaedic Surgery, Shanghai Jiao Tong University Affiliated Sixth People's Hospital, Shanghai, People's Republic of China

[2] Department of Orthopaedics & Traumatology, Stem Cells and Regeneration Laboratory, Li Ka Shing Institute of Health Sciences, Faculty of Medicine, Prince of Wales Hospital, The Chinese University of Hong Kong, Room 904, 9/F, Shatin, Hong Kong Sar, People's Republic of China

[3] Institute of Orthopedic Diseases and Department of Orthopedics, the First Affiliated Hospital, Jinan University, Guangzhou, People's Republic of China

Neovascularization is an important factor in bone healing, especially during the DO process, and it involves the rapid migration of endothelial progenitor cells (EPCs) and mesenchymal stem cells (MSCs), and their homing and differentiation, contributing to the formation of primitive tubular vessel structures [2, 5–7]. The sprouting and remodeling of blood vessels from the existing vasculature and the subsequent formation of new tissue have been suggested to be crucial for successful distraction osteogenesis [8]. These processes cooperatively promote angiogenesis and osteogenesis through a key stem cell homing factor, stromal cell-derived factor-1 (SDF-1) [8]. SDF-1 was first identified as a soluble ligand secreted by bone marrow stromal cells, and it belongs to the CXC subfamily of chemokines and plays a major role in angiogenesis [9]. CXCR4 is a seven-pass G protein-coupled transmembrane receptor for SDF-1, expressed on the surface of MSCs and bone marrow stromal cells [10]. The crucial role of SDF-1/CXCR4 signaling during development has been demonstrated in heart and nervous systems [11]. In bones, SDF-1 can stimulate chondrocyte hypertrophy, regulate bone marrow protein (BMP) 2-stimulated osteogenic differentiation, mediate EPC differentiation through the enhancement of cell adhesion, and promote early osteoclast differentiation [12–14]. Moreover, SDF-1 is rapidly upregulated at the sites of ischemic tissue damage, and it attracts circulating CXCR4-expressing MSCs, assisting the process of tissue repair [15, 16]. The inhibition of SDF-1/CXCR4 signaling was demonstrated to attenuate fracture healing [17]. Taken together, SDF-1/CXCR4 signaling may play a crucial role in bone regeneration.

In this study, we compared the expression of SDF-1 and early osteogenic markers during tibial DO and fracture healing in rats. Afterward, we examined the roles of SDF-1/Cxcr4 signaling in bone regeneration, by locally applying a Cxcr4 antagonist, AMD3100 [18], to rats undergo DO procedure. Furthermore, we investigated the effect of AMD3100 on osteogenic differentiation of rat bone marrow mesenchymal stem cells (rBMSCs), in order to determine the potential beneficial approaches modulating Cxcr4 and SDF-1 signaling pathway during bone regeneration in DO treatment.

Materials and Methods

Animals

Three-month-old male Sprague–Dawley rats were obtained from the Laboratory Animal Services Centre of the Chinese University of Hong Kong ($n=5$ for rBMSCs harvest; $n=3$ for normal bone harvest; $n=15$ for fracture model; $n=35$ for DO model). All rats were housed in plastic cages at 25 ± 1 °C and constant humidity and had free access to standard laboratory chow and sterile water.

Rat Fracture Model

Fifteen rats (belonging to the fracture group) were anesthetized using xylazine (4 mg/kg) and ketamine (40 mg/kg), administered intraperitoneally. A mid-diaphysis transverse osteotomy was performed on the right tibia under sterile conditions. A monolateral external fixator/lengthener (Xinzhong Medical Device Company, Tianjin, PR China) was assembled to fix two segments with four stainless steel pins, followed by the sequential suture of the incision. Animals belonging to the fracture group were sacrificed at day 5, 10, 15, 29, and 43 ($n=3$ at each time point) after surgery. At day 0, normal tibia segments from three rats belonging to the control group were harvested.

Rat DO Model

A total of 35 rats were operated under general anesthesia and sterile conditions [19]. The surgical procedure was the same as previously described for the rats belonging to the fracture group. Following a 5-day latency period, lengthening was initiated and maintained at a rate of 0.25 mm/12 h for 10 days, and the total lengthening was 5 mm. After the lengthening completed, the position of bone segments was maintained by the external fixator/lengthener for another 4 weeks before termination. Fifteen rats designated as DO group were used for comparison with the fracture group. Rats were sacrificed at day 5, 10, 15, 29, and 43 ($n=3$ at each time point) after surgery. The remaining twenty rats were randomly divided into two groups: phosphate-buffered saline (PBS) group ($n=10$) and AMD3100 (Sigma-Aldrich, St. Louis, MO, USA) group ($n=10$). From the initiation of the lengthening period, animals were injected with either 100 µL of PBS or 100 µL of AMD3100 solution (at a concentration of 400 µM in PBS) into the distraction gap every 2 days until their termination. AMD3100 was used at the concentration of 400 µM in PBS, which was shown to inhibit SDF-1/Cxcr4 signaling effectively, without causing toxicity [12, 20]. Calcein (10 mg/kg) and xylenol orange (30 mg/kg) (Sigma-Aldrich, St Louis, MO, USA) were subcutaneously injected into the rats at day 16 and day 40 following initial surgery, respectively. At termination, bilateral tibias were harvested by removing the fixators at day 43 after the surgery, for further analyses.

Detection of SDF-1 Expression

After termination, the segments of the callus were removed in animals in the fracture and DO groups, weighed, and kept in liquid nitrogen until further use. Enzyme-linked

immunosorbent assay (ELISA; Shanghai LanPai Biotechnology Co., Ltd) was used to detect the expression of SDF-1, and the obtained measurements were normalized to the weight of each segment, according to the manufacturer's protocol.

Bone RNA Extraction and Real-Time PCR

Five days after the distraction, total RNA was isolated using TRIzol (Life Technologies, USA) from the regenerate tissues in each rat after homogenization with liquid nitrogen, and the RNA was reverse-transcribed with PrimeScript RT Reagent Kit (Takara, Japan), according to the manufacturer's instructions. Real-time PCR was performed with SYBR Green PCR Master Mix (Applied Biosystems, USA). Osteogenic gene primer sequences are listed in Table 1. *Gapdh* was used as an internal control, in order to evaluate the relative expression, and the changes were quantified using the delta–delta Ct method.

Digital Radiography

At the end of the distraction phase, anterior–posterior X-ray images including the distraction zone were obtained weekly under general anesthesia until the sacrifice. A digital X-ray machine (MX-20, Faxitron X-Ray Corp., Wheeling, IL, USA) was used, with the exposure time of 6000 ms and a voltage of 32 kV.

Micro-computed Tomography (μCT) Analysis of the Regenerating Tissue

Structural changes within the distraction zone in the DO rats ($n=8$) were quantitatively assessed using a high-solution μCT40 scanner (SCANCO Medical, Bassersdorf, Switzerland) at the termination. Three-dimensional (3D) reconstruction of the mineralized tissues was performed by applying a global threshold (165 mg hydroxyapatite/cm^3), and a Gaussian filtering ($\sigma=0.8$, support$=2$) was used to suppress background noise. The middle 200 layers in the horizontal plane of the distraction zone were selected as our region of interest. Using different thresholds (low attenuation $n=158$, high attenuation $n=211$), low- and high-density mineralized tissues, representing newly formed callus and highly mineralized bones, respectively, were reconstructed according to an established protocol [21]. Bone mineral density (BMD), bone volume/total tissue volume (BV/TV), Tb.N (trabecular number), Tb.Th (trabecular thickness), Tb.Sp (trabecular separation), and connected density (Conn-Dens) were determined using the built-in software.

Four-Point Bending Mechanical Test

This mechanical test was performed within 24 h after termination at room temperature. A four-point bending device (H25KS; Hounsfield Test Equipment, Surrey, UK) with a 250-N load cell was used to test tibial failure in the anterior–posterior direction with the inner and outer span of the blades set to 8 and 18 mm, respectively. The long axis of the tibia was oriented perpendicular to the blades during the tests. A load was constantly applied to the distraction zone at a displacement rate of 5 mm/min. The modulus of elasticity (E-modulus), ultimate load, energy to failure, and maximum stress were recorded with QMAT Professional software (Tinius Olsen, Horsham, PA, USA). The contralateral tibia was used as an internal control ($n=8$ per group).

Histological Analyses

Following the animal termination, bone specimens ($n=3$ per group) were dehydrated in a graded series of alcohol and xylene and embedded in methyl methacrylate. Each sample was cut in half with a SP1600 saw microtome (Leica, Nussloch, Germany) along the long axis of the tibia in the midsagittal plane, and 5- and 10-μm-thick sections were cut with an RM2155 hard tissue microtome (Leica, Wetzlar, Germany) along the long bone axis. The 5-μm sections were stained with Von Kossa, Safranin O, Masson's Trichrome, and Goldner's Trichrome stains, in order to perform static histomorphometric analysis, while unstained

Table 1 Primer sequences used in quantitative real-time PCR analyses

Gene name	Forward primer sequence (5′–3′)	Reverse primer sequence (5′–3′)	Product size (bp)
Glyceraldehyde-3-phosphate dehydrogenase (GAPDH)	CGGCAAGTTCAACGGCACAG	GAAGACGCCAGTAGACTCCACGAC	148
Alkaline phosphatase (ALP)	GGACAATGAGATGCGCCC	CACCACCCATGATCACATCG	101
Runt-related transcription factor 2 (Runx2)	AAGGTTGTAGCCCTCGGAGA	TTGAACCTGGCCACTTGGTT	128
Osteopontin (Opn)	GGCTGAATTCTGAGGGACCAA	GCTGTAATGCGCCTTCTCCT	131

10-μm sections were used for dynamic histomorphometric measurements, performed using a fluorescence microscope (DMRXA2; Leica). Bone analysis software, OsteoMeasure (Osteometrics, Decatur, GA, USA), was used to analyze the obtained parameters, including the ratio of mineralized surface to bone surface (MS/BS), mineral apposition rate (MAR), bone formation rate per unit of bone surface (BFR/BS), bone formation rate per bone volume (BFR/BV), and bone formation rate per TV (BFR/TV).

Isolation and Culture of rBMSCs

rBMSC isolation and culturing were described previously [19]. Briefly, bone marrow of 12-week-old Sprague Dawley rats was flushed out from the femoral cavity and cultured in the complete α-modified Eagle's medium (α-MEM, Invitrogen, USA) at 37 °C in the atmosphere containing 5% CO_2 and with 95% humidity. rBMSCs from passages 3–5 were used in further experiments. Surface markers, including CD34, CD44, CD45, and CD90 were used to determine the purity of cells by flow cytometry.

Immunofluorescence Staining

Nestin- and Cxcr4-positive cells were determined by immunofluorescence staining. rBMSCs were incubated in 12-well plates at a concentration of 10,000 cells/cm^2. After 24 h, cells were fixed with 4% paraformaldehyde for 10 min and permeabilized with 0.1% Triton-X 100 for 5 min. Following their blocking with 5% normal goat serum for 30 min, we incubated the cells with primary antibodies against rabbit Nestin (Sigma, 1:300, N5413) or mouse Cxcr4 (R&D., 1:300, N5413) overnight at 4 °C. Afterward, the cells were incubated with the Alexa Fluor 488-conjugated secondary antibody (Invitrogen Corporation, Carlsbad, CA, USA) for 1 h at room temperature. Mounting solution containing 1 μg/mL DAPI (Sigma-Aldrich) was used to stain the cell nuclei.

Osteogenic Differentiation

Briefly, after cells seeded in 12-well plate reached over 80% confluence, α-MEM was replaced with osteogenic induction medium (OIM; 100 nmol/L dexamethasone, 0.05 mmol/L l-ascorbic acid-2-phosphate, and 20 mmol/L β-glycerophosphate with complete α-MEM). In order to block SDF-1/Cxcr4 signaling in primary rBMSCs, AMD3100 (400 μM) was added into OIM. OIM without AMD3100 and α-MEM were used as positive and negative controls, respectively. Media were replaced every 3 days. All experiments were performed in triplicates.

Alkaline Phosphatase (ALP) Staining

Three days after seeding, rBMSCs were equilibrated twice by using ALP buffer (0.1 M NaCl, 0.1 M Tris–HCl, 50 mM $MgCl_2{\cdot}6H_2O$; pH 9.5) for 5 min, incubated with ALP substrate solution (5 μL BCIP and 10 μL NBT in 1 mL ALP buffer) at 37 °C in dark for 60 min, and the reaction was stopped by distilled water. Plates were dried before obtaining the images.

Alizarin Red S Staining

Fourteen days after seeding, rBMSCs were stained with Alizarin Red S (pH 4.2) for 10 min at room temperature, and washed with distilled water. The monolayer was eluted with 10% cetylpyridinium chloride (CPC) to quantify the mineralization, and the optical density (OD) of the extract was measured at 570 nm.

Cellular RNA Extraction and Real-Time PCR

After 7 days of incubation, total cellular RNA was isolated using TRIzol (Life Technologies, USA) and it was reverse-transcribed with PrimeScript RT Reagent Kit (Takara, Japan). The method was the same as that applied for bone RNA extraction.

Statistical Analysis

All quantitative data were transferred to statistical spreadsheets and analyzed using SPSS 18.0 software for Windows (SPSS, Chicago, IL, USA). Mann–Whitney U test with a Bonferroni correction was performed for the comparison of mean values, and $p < 0.05$ was considered statistically significant.

Results

Expression of SDF-1 and Early Osteogenic Markers in DO and Fracture Groups

At day 5, bone segments of the rats belonging to different groups were harvested. No significant difference in SDF-1 concentration between the DO and fracture groups was observed ($p > 0.05$). In the fracture group, the expression of SDF-1 remained at the baseline level following the surgery, and no significant change in the expression levels was observed over time, compared with the control group. In the DO group, SDF-1 expression increased by $234.4 \pm 57.5\%$ at day 15 after the surgery (end of the distraction phase) and remained higher than that of the control group. At day 29 and 43, SDF-1 expression in the

distraction zones was significantly higher than that in the fracture zones ($p < 0.05$) (Fig. 1a). However, at the early phase of distraction (10 days after surgery), there was no difference in SDF-1 expression levels between the DO and fracture groups. For further identification, the expression levels of early osteogenic markers, ALP, Runx2, and Opn, and SDF-1 in callus were determined, and it was shown that the expression of all these markers was significantly upregulated in the DO group, compared with those in the control and fracture groups (Fig. 1b).

Radiographic Assessments

Weekly X-ray images of each rat in the DO group, treated with AMD3100 or PBS, were obtained (Fig. 2a). The representative images presented in Fig. 2b demonstrate the progression of bone consolidation. Although the rate of new callus formation increased with time in both groups, the quality of the newly mineralized bone in terms of the volume of the regenerating tissue was considerably decreased in AMD3100 group than that in the PBS group (Fig. 2b).

µCT Analyses of the Distraction Regenerates

The 3D reconstructed µCT images show that the continuity of the regenerates was not complete in the AMD3100 group (Fig. 3a). Considerable differences in the parameters obtained by using the µCT analysis were observed as well. The BMD values of the distraction zone in the AMD3100 group (328.8 ± 37.9 mg/cm^3) significantly decreased in comparison with those in the PBS group (381.4 ± 30.1 mg/cm^3) (Fig. 3b). Similarly, BV/TV values were shown to be considerably downregulated after AMD3100 administration in all three thresholds (158–211, 0.15 ± 0.05; 158–1000, 0.49 ± 0.09; 211–1000, 0.35 ± 0.05), compared with those in the PBS-treated animals (158–211, 0.22 ± 0.04; 158–1000, 0.62 ± 0.07; 211–1000, 0.40 ± 0.04) (Fig. 3c). Furthermore, Tb.N values in all three thresholds were lower in the AMD3100 group (158–211, 1.51 ± 0.52 mm^{-1}; 158–1000, 1.29 ± 0.41 mm^{-1}; 211–1000, 1.08 ± 0.38 mm^{-1}) than in the PBS group (158–211, 2.35 ± 0.37 mm^{-1}; 158–1000, 1.92 ± 0.29 mm^{-1}; 211–1000, 1.63 ± 0.31 mm^{-1}) (Fig. 3d), and Tb.Th values in the AMD3100 group (158–211, 0.07 ± 0.02 mm; 158–1000, 0.41 ± 0.04 mm) were significantly lower in 158–211 and 158–1000 thresholds, in comparison with those in the PBS group (158–211, 0.10 ± 0.02 mm; 158–1000, 0.46 ± 0.04 mm) (Fig. 3e). However, in the AMD3100 group (158–211, 0.74 ± 0.21 mm; 158–1000, 1.03 ± 0.33 mm; 211–1000, 1.16 ± 0.34 mm), Tb.Sp values in all three thresholds significantly increased in comparison with those in the PBS group (158–211, 0.46 ± 0.07 mm; 158–1000, 0.58 ± 0.13 mm; 211–1000, 0.70 ± 0.14 mm) (Fig. 3f). Conn-Dens values in 158–211 threshold were shown to be higher in the AMD3100 group (35.84 ± 5.83 mm^{-3}) compared with those in the PBS group (27.80 ± 3.76 mm^{-3}) (Fig. 3g).

Mechanical Properties of the Distraction Regenerates

E-modulus, ultimate load, and maximum stress values were shown to be significantly decreased following the administration of AMD3100 (33.7 ± 13.2 MPa, 48.1 ± 19.6 N, 24.0 ± 9.8 N/mm, respectively), compared with these

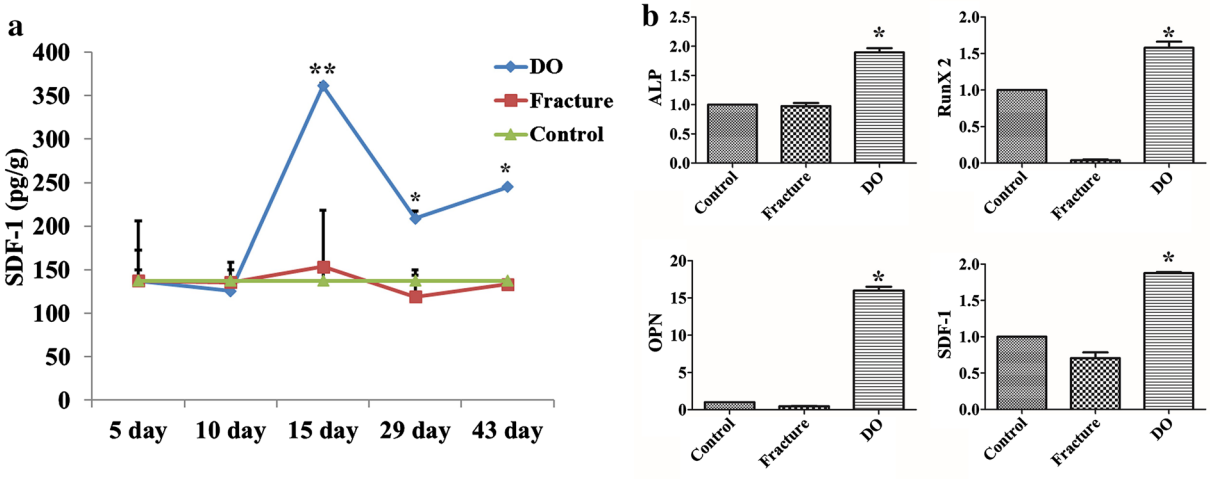

Fig. 1 Expression of SDF-1 and early osteogenic markers in the DO and fracture sites. **a** ELISA results, showing that SDF-1 expression at different time points in the DO and fracture groups. **b** Real-time PCR results, showing the expression of SDF-1 and early osteogenic markers, including ALP, Runx2, and Opn in new callus of the DO, control, and fracture groups. *$p < 0.05$, compared with the fracture group ($n = 3$ in each group)

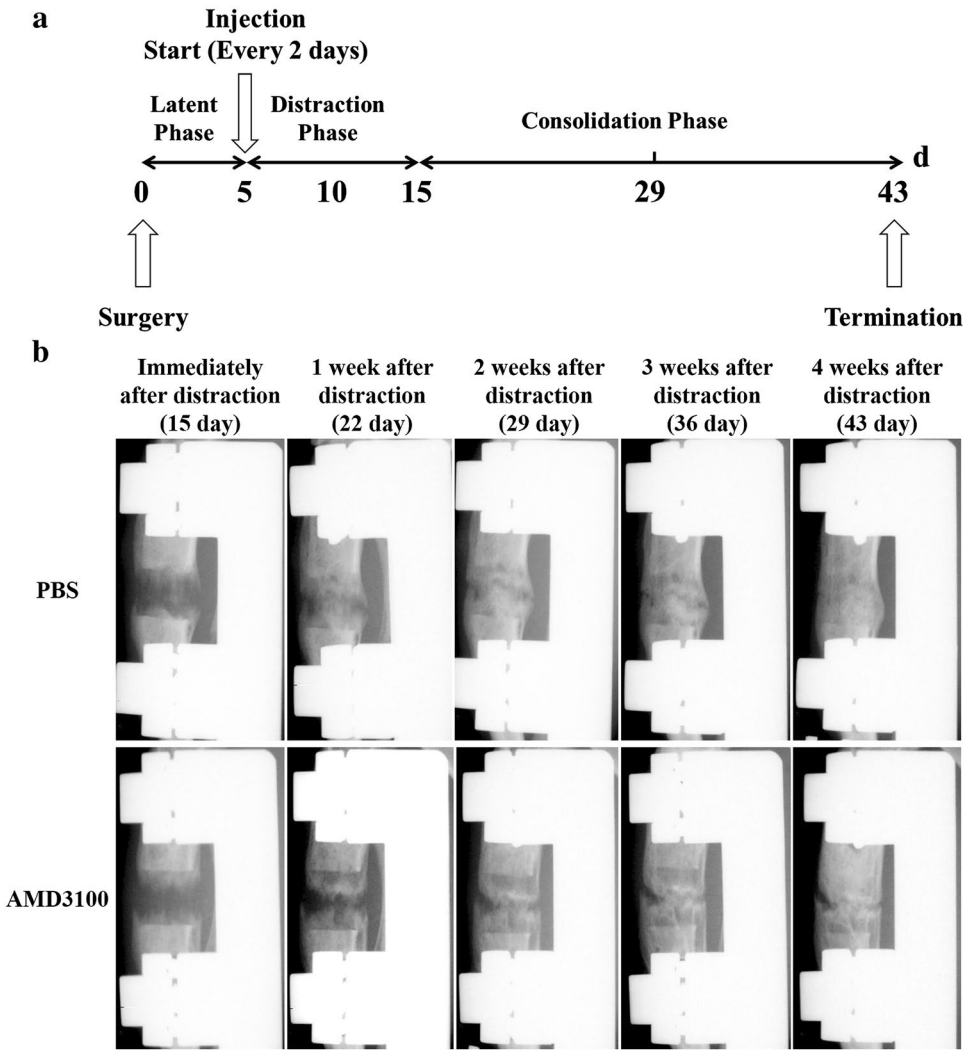

Fig. 2 Experimental design and representative X-ray images of the DO rats. **a** After a 5-day latency period, lengthening was initiated at 0.25 mm/12 h for 10 days. PBS and AMD3100 were locally administrated from the beginning of the distraction phase until the animal sacrifice (43 days after surgery), every 2 days. **b** X-ray images, showing bone consolidation and the quality of the newly mineralized bone ($n = 10$ in each group)

values measured after PBS treatment (66.7 ± 6.9 MPa, 74.9 ± 11.0 N, 37.4 ± 5.5 N/mm, respectively). No significant difference in the energy to failure values between two groups was observed ($p > 0.05$) (Fig. 4; Table 2).

Histological Assessments of the Newly Formed Bones in Rats with DO Treatments

Undecalcified sections obtained from the rats in each group at day 43 after surgery were stained with Von Kossa, Safranin O, Goldner's Trichrome, and Masson's Trichrome stains. Following the Von Kossa staining, the newly formed calluses were shown to be almost consolidated in the PBS group, whereas the callus formation was still ongoing, with rare signs of bone remodeling at the center of the regenerate in the AMD3100 group (Fig. 5a, b). Safranin O staining demonstrated that chondrocytes (cartilage) were still observable in the AMD3100 group, unlike in the PBS-treated animals (Fig. 5c, d). Goldner's Trichrome and Masson's Trichrome staining showed the presence of bone marrow cavities in the PBS group (Fig. 5e-h).

The dynamic bone formation in distraction regenerates is presented in Fig. 6. The distance between the green (calcein) line and the red (xylenol orange) line indicates the speed of new callus mineralization. In comparison with the PBS group, the bone formation rate was obviously decreased after the administration of AMD3100 (Fig. 6a). Quantitative measurements including MS/BS, MAR, BFR/BS, BFR/BV, and BFR/TV values, were significantly decreased in the AMD3100 group, compared with those in the PBS group (Fig. 6b).

SDF-1/Cxcr4 Signaling During rBMSC Osteogenic Differentiation

Immunofluorescence staining demonstrated that Nestin-positive rBMSCs (green) express Cxcr4 (red), the SDF-1 receptor (Fig. 7). To clarify the effect of the osteogenic differentiation of rBMSCs in vitro, ALP and Alizarin

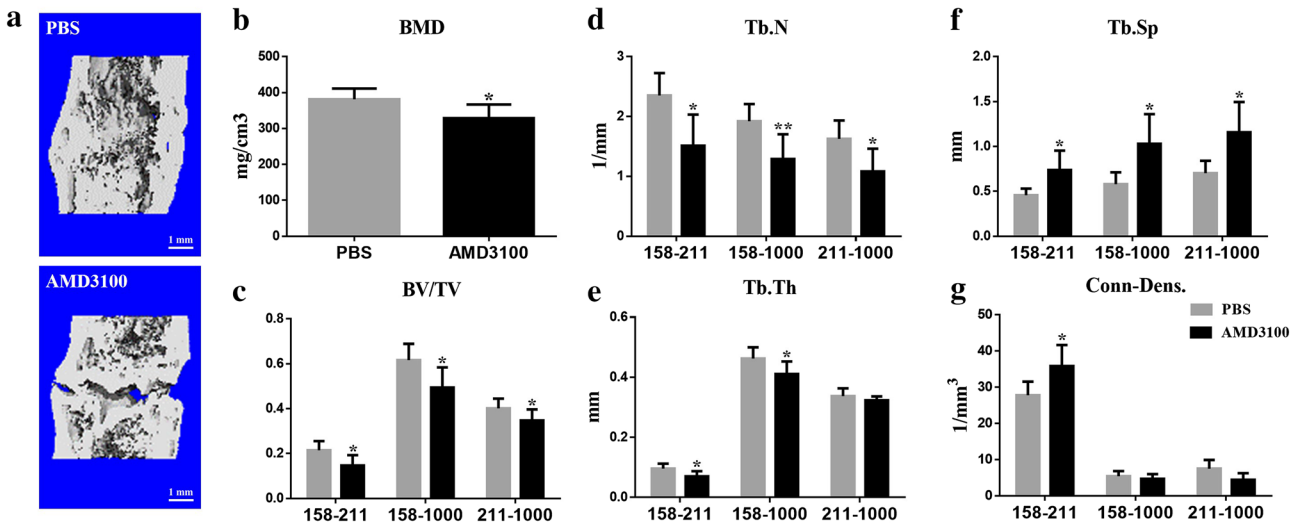

Fig. 3 Bone consolidation following the AMD3100 administration. **a** 3D μCT images of distraction regenerating tissue, showing less mineralized bone in the AMD3100 group. **b** BMD in the AMD3100 group, significantly decreased in comparison with that in the PBS group. **c, d** BV/TV and Tb.N values in AMD3100 and PBS-treated animals. **e** Tb.Th values, measured in the AMD3100 and PBS-treated groups. **f** Tb.Sp values, determined in the AMD3100 and PBS groups. **g** Conn-Dens values, measured in the AMD3100 and PBS treatment groups ($n=8$ per group)

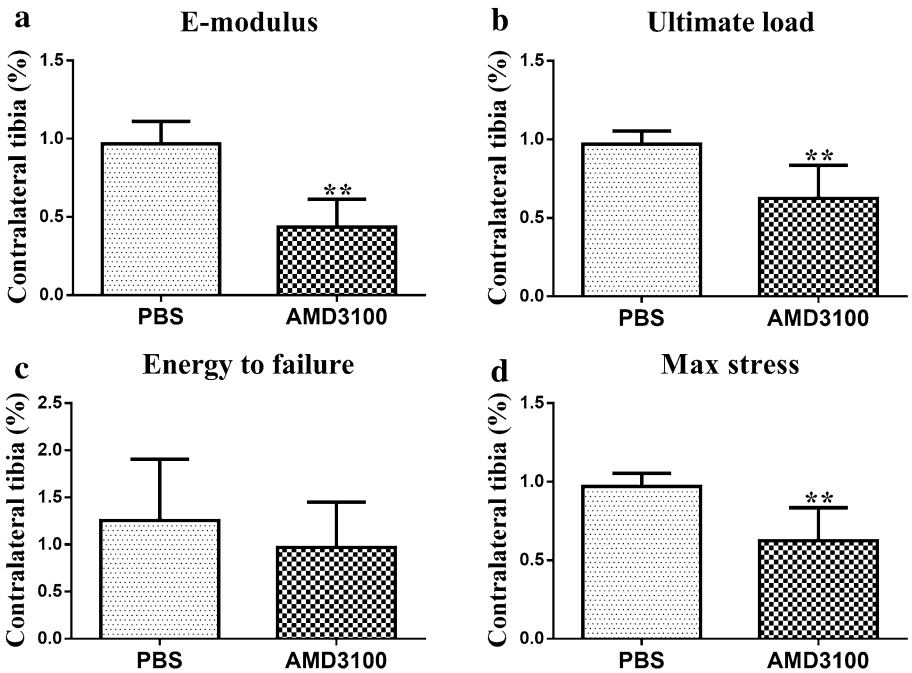

Fig. 4 Mechanical properties of the regenerating tissues. E-modulus (**a**), ultimate load (**b**), and maximum stress (**d**) values were significantly decreased after AMD3100 administration, and no significant difference in energy to failure (**c**) levels was observed between two groups. *$p<0.05$ ($n=8$ per group)

Table 2 Mechanical properties of the distraction regenerating tissue

	E-modulus (MPa)	Ultimate load (N)	Energy to failure (J)	Max stress (N/mm)
PBS	66.65 ± 6.91	74.85 ± 10.95	0.0320 ± 0.0103	37.42 ± 5.48
AMD3100	33.66 ± 13.19**	48.09 ± 19.62*	0.0228 ± 0.014	24.05 ± 9.82*

*$p<0.05$, **$p<0.01$, compared to the PBS group ($n=8$ in each group)

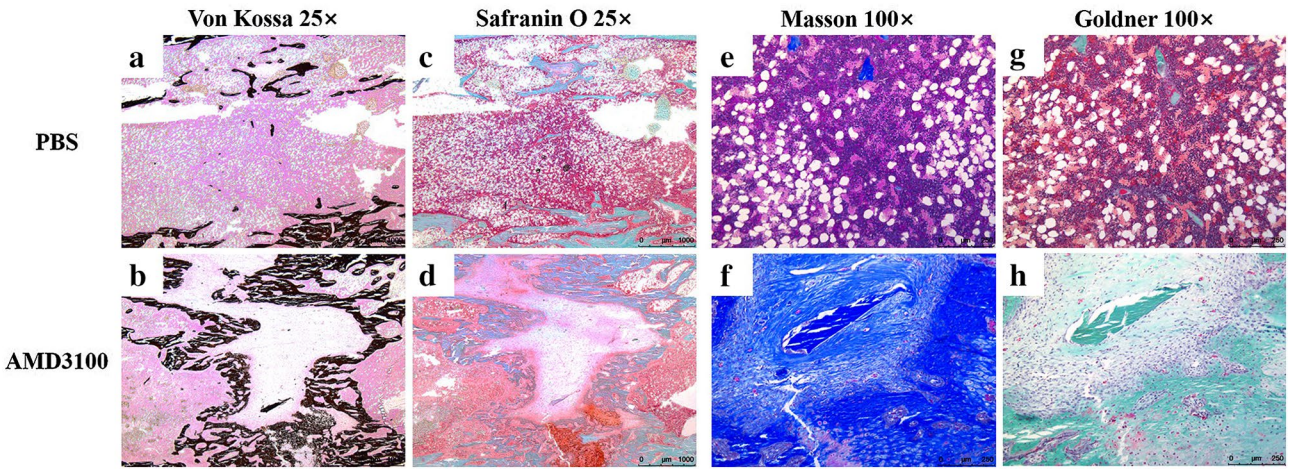

Fig. 5 AMD3100 administration led to the inhibition of new callus consolidation. **a, b** Von Kossa staining showed many newly formed calluses in AMD3100-treated animals, while the continuity of the cortical bone was evident in the PBS group. **c, d** Safranin O staining, showing increased areas of cartilage in the AMD3100 group, in comparison with the PBS group. **e–h** Masson's and Goldner's Trichrome staining, showing the continuity of bone marrow cavities in the PBS group, but not in the AMD3100 group

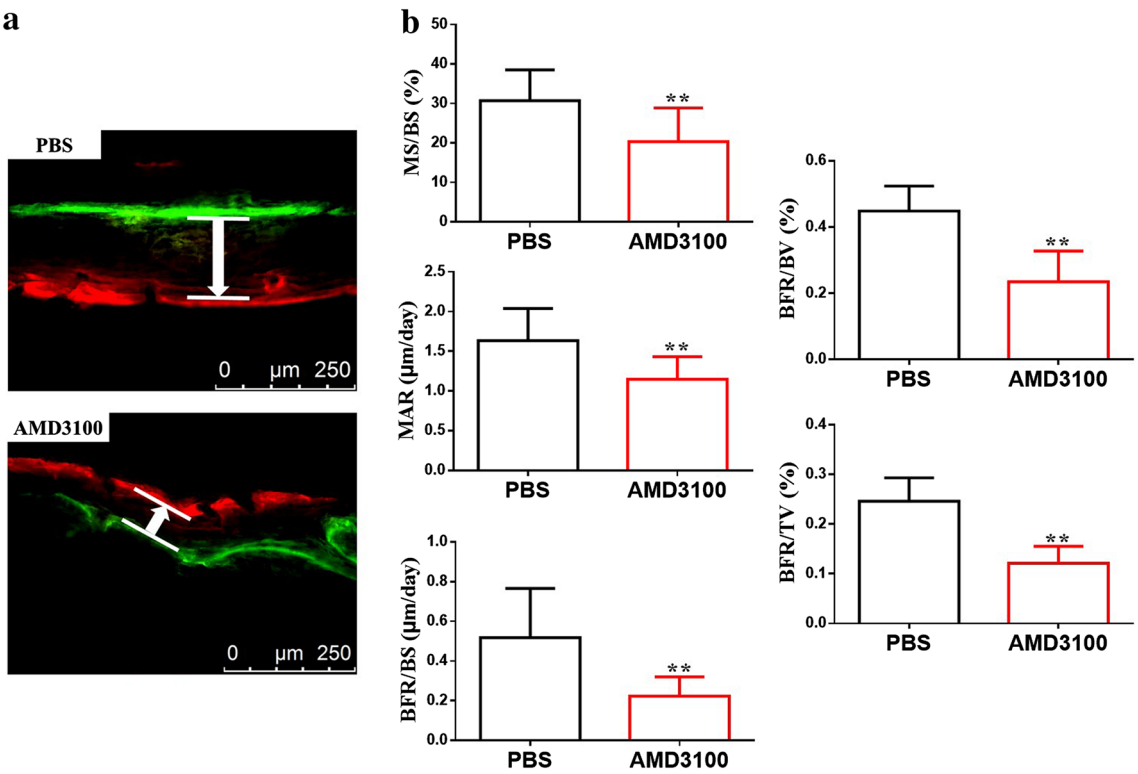

Fig. 6 AMD3100 administration leads to the decreased rate of bone formation. **a** The distance from the *green* (calcein) *line* to the *red* (xylenol *orange*) one indicates the speed of new bone formation in AMD3100 and PBS groups. **b** Dynamic histomorphometric parameter (*MS/BS, MAR, BFR/BS, BFR/BV*, and *BFR/TV*) values in AMD3100 and PBS-treated animals. $^{**}p < 0.01$, compared with the PBS group. (Color figure online)

Red S staining were performed at day 3 and day 14 after the initiation of osteogenic differentiation, respectively. The expression of ALP and the amount of calcium deposits were markedly increased after the incubation of these cells in OIM, compared with those in the α-MEM. After AMD3100 treatment, ALP expression at day 3 significantly decreased, compared with that in the OIM-induced cells, while no difference in the calcium deposit levels at day 14

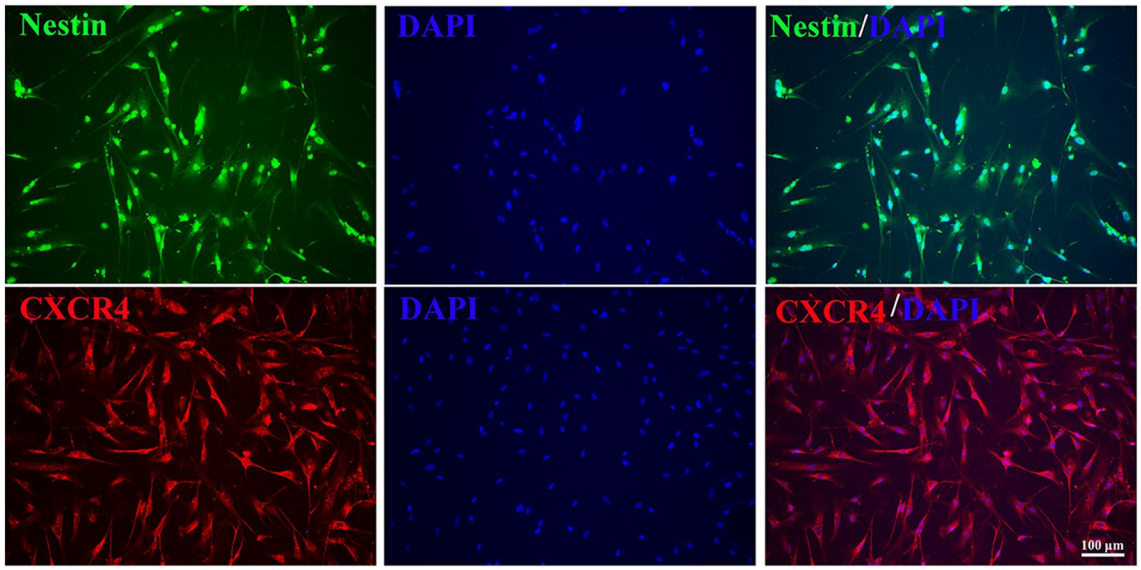

Fig. 7 Immunofluorescence staining, showing that MSCs isolated from rat bone marrow were Nestin-positive (*green*) and expressed Cxcr4 (*red*). The nuclei were stained with DAPI (*blue*). (Color figure online)

was seen between the two groups (Fig. 8a). Furthermore, real-time PCR results showed a considerable decrease in ALP, Runx2, and Opn after AMD3100 treatment of the cells maintained in OIM, compared with the cells in OIM alone (Fig. 8b).

Discussion

Here, we demonstrated that the expression of SDF-1 is increased in the regenerate in DO process, compared with that in the fracture-healing process, especially during the distraction phase. Additionally, we examined the effects of the local administration of SDF-1/Cxcr4 signaling antagonist AMD3100 on the mineralization of new bone in the DO gap. AMD3100 was shown to inhibit DO-mediated tissue regeneration and rBMSC osteogenic differentiation, demonstrating a crucial role of SDF-1/Cxcr4 signaling during bone regeneration.

The potential enhancements of new bone formation during DO have been reviewed recently [22], most of these interventions focused on the downstream effectors of complex molecular/physiological mechanisms, in order to accelerate bone consolidation. Upstream factors, such as those involved in the processes of neovascularization, during which the SDF-1/Cxcr4 signaling plays a critical role [23], may also be potential therapeutic targets. Previously, tissue hypoxia was observed during bone healing [17], and the expression of SDF-1 was increased in hypoxic tissues [24]. The regulation of neovascularization in distraction tissues is associated with the increased levels of hypoxia-inducible factor 1α (HIF-1α) in the regenerate tissues, in comparison with those in the fracture calluses [2, 25]. The recruitment of CXCR4-positive progenitor cells, such as EPCs and MSCs, to regenerating tissues is mediated by hypoxic gradients via HIF-1α-induced expression of SDF-1 [25], which explains the increased expression of SDF-1 in DO callus observed in our experiments. Three well-known phases can be observed during DO process, including latency, distraction, and consolidation. During the distraction phase, the callus is stretched gradually to the maximum extent. The expression of HIF-1α-induced SDF-1 in the ischemic gap-tissue increased gradually, and peaked at the end of the distraction phase, which was followed by a marked increase in blood flow and vascular proliferation that continued throughout the consolidation phase [26]. Together with SDF-1 expression, the expression levels of early osteogenic markers, including ALP, Runx2, and Opn, in DO were markedly upregulated as well when mechanical strain was applied.

SDF-1 inhibition in the regenerating tissue or Cxcr4 inhibition in the progenitor cells may prevent cell recruitment to the ischemic sites [24]. Therefore, to confirm the role of SDF-1/Cxcr4 signaling in the DO process, AMD3100 was injected locally into the regenerating tissue, and the reduction of total new bone volume in AMD3100-treated rats was observed. Similarly, μCT data showed significant differences in the measured parameters between the PBS-treated and the AMD3100-treated animals. Four-point bending tests demonstrated that the mechanical properties of the regenerates considerably decreased after AMD3100 administration, while histomorphometric callus analyses

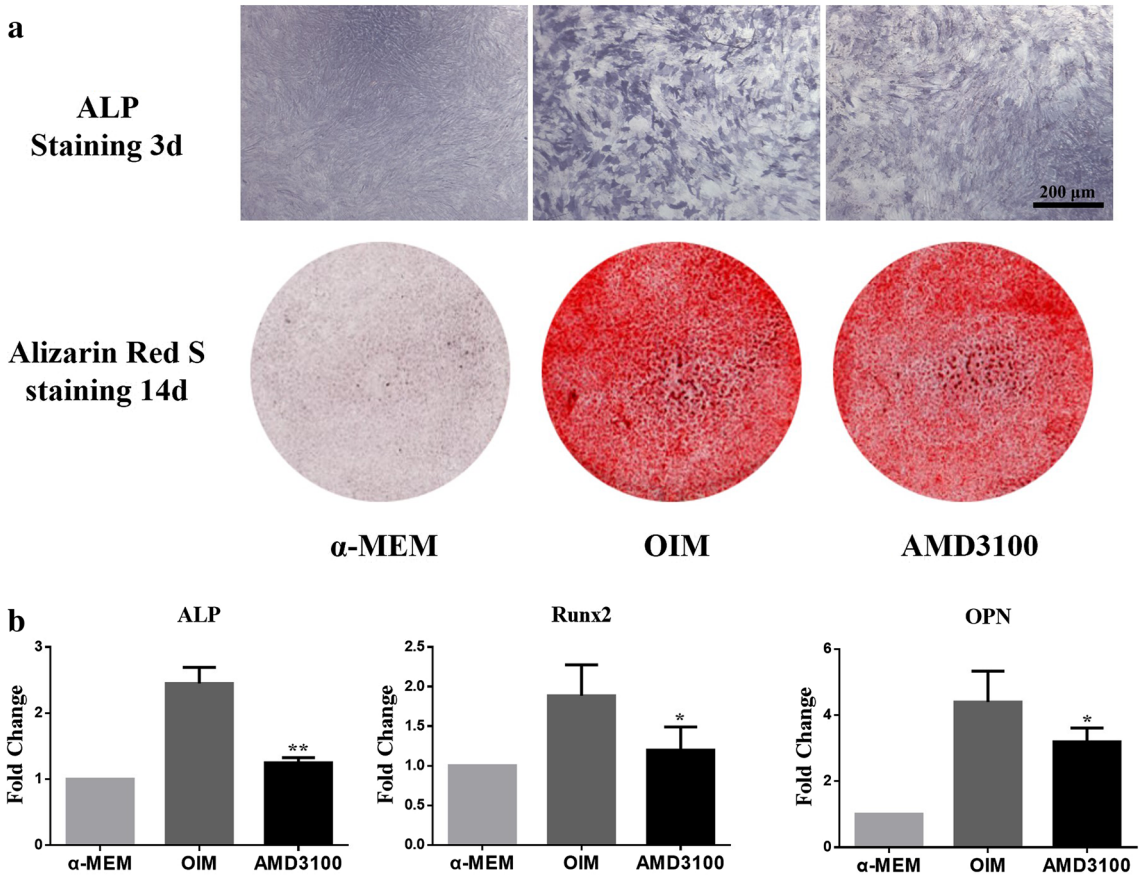

Fig. 8 The role of SDF-1/Cxcr4 signaling in rBMSC osteogenic differentiation. **a** ALP staining at day 3 after AMD3100 administration, showing a decreased expression of ALP. Alizarin Red S staining at day 14 after AMD3100 administration showed no difference in the rate of calcium deposit formation between the groups. **b** The expression early osteogenesis-related genes (*ALP, Runx2*, and *Opn*), significantly downregulated after AMD3100 administration. All experiments were performed in triplicates. $*p<0.05$, $**p<0.01$, compared with the OIM group

revealed that chondrocytes and fibroblasts were still seen in the distraction gap 4 weeks after the initiation of distraction in AMD3100 group, and some newly formed chondrocytes have not been mineralized completely after AMD3100 injection, whereas the new bone is completely mineralized and the bone marrow cavity was almost re-connected (demonstrating rapid bone remodeling) in the control group. Dynamic histomorphometric data showed that the speed of new bone mineralization was significantly less in the AMD3100 treated group in comparison to the PBS injection group.

In several studies, AMD3100 was reported as a hematopoietic stem cell mobilizer, which were administrated intraperitoneally to mobilize the circulating progenitor cells and to improve neovascularization and osteogenesis associated with enhanced bone healing [23, 27]. In a related study from Toupadakis et al. [17], it was suggested that a long-term local administration of AMD3100 can significantly hinder fracture repair. As demonstrated by Kitaori et al. [28], SDF-1 expression was induced in the periosteum of injured bone, which promoted endochondral bone repair by recruiting MSCs to the ischemic tissues. AMD3100, SDF-1/Cxcr4 signaling antagonist, significantly attenuated load-induced periosteal bone formation [29], and therefore, during DO process the regeneration of the weight-bearing long bones may be inhibited by AMD3100 treatment.

The interruption of SDF-1/Cxcr4 signaling may also affect osteogenic differentiation of rBMSCs. Granero-Moltó et al. [30] showed that MSCs homing to the fracture site was exclusively time-dependent and Cxcr4 dose-dependent. Here, we isolated rBMSCs from the rat bone marrow and showed that they expressed Cxcr4. We demonstrated that the inhibition of the SDF-1/Cxcr4 signaling during the osteogenic differentiation of rBMSCs with AMD3100 treatment led to a significant decrease in ALP activity, and reduced the expression of osteogenesis-related genes, which are the indicators of early-stage osteogenic differentiation [20]. Luan et al. [31] reported an inhibitory

effect of AMD3100 on osteogenic differentiation of MC3T3-E1 cells, especially in the early stage of this process. Furthermore, the addition of exogenous SDF-1 does not affect calcium deposition rate, which represents a late osteogenic marker, and SDF-1/Cxcr4 exert their functions in the early and middle stages of osteogenic differentiation through the activation of Smad and MAPK signaling pathway [20]. In this study, we obtained similar results and no significant difference in the formation of calcium nodules was observed between the groups. SDF-1/CXCR4 signaling was shown to be a key axis linking EPCs, BMSCs, osteoblasts, and osteoclasts during the normal homeostatic regulation of bone regeneration and remodeling [13, 14].

The limitation of this study is that the detailed molecular mechanisms determining the degree of consolidation after the administration of AMD3100 remain unclear. In agreement with the results obtained in previous studies, an increased number of progenitor cells recruited by SDF-1 lead to the expression of multiple pro-angiogenic factors in the DO gap during the distraction phase, and this is associated with an increased rate of vascularization, compared with that observed at the fracture site during the immediate-early phase of healing [5, 26]. The inhibition of SDF-1/Cxcr4 signaling by AMD3100 may affect the migration and differentiation of progenitor cells and neovascularization in the distraction regenerate; further investigations are required to confirm SDF-1-mediated angiogenesis and osteogenesis.

In conclusion, DO process promotes an increase in SDF-1 expression. Local application of SDF-1/Cxcr4 signaling antagonist AMD3100 may significantly hinder bone mineralization and rBMSC osteogenic differentiation. These findings may suggest novel therapeutic manipulation of osteoprogenitor cell homing and differentiation, to induce bone consolidation in patients undergoing DO treatment.

Acknowledgements The work was partially supported by grants from National Natural Science Foundation of China (NSFC Nos. 81371946, 81374568), Hong Kong Government Research Grant Council, General Research Fund (CUHK470813 and 14119115), and a project grant from China Shenzhen City Science and Technology Bureau (JGJHZ20140419120051680 and JCYJ20150630165236960) to Gang Li. This study was also partly supported by SMART program, Lui Che Woo Institute of Innovative Medicine, The Chinese University of Hong Kong.

Compliance with Ethical Standards

Conflict of interest Jia Xu, Yuanfeng Chen, Yang Liu, Jinfang Zhang, Qinglin Kang, Kiwai Ho, Yimin Chai, and Gang Li declare that they have no conflict of interest.

Human and Animal Rights and Informed Consent All animal experiments were carried out under the animal license issued by the Hong Kong SAR Government and the approval of the Animal Experimentation Ethics Committee of the Chinese University of Hong Kong (Ref No. 14-052-MIS).

References

1. Ilizarov GA (1990) Clinical application of the tension-stress effect for limb lengthening. Clin Orthop Relat Res 250:8–26
2. Ai-Aql ZS, Alagl AS, Graves DT, Gerstenfeld LC, Einhorn TA (2008) Molecular mechanisms controlling bone formation during fracture healing and distraction osteogenesis. J Dent Res 87(2):107–118
3. Ilizarov GA (1989) The tension-stress effect on the genesis and growth of tissues. Part I. The influence of stability of fixation and soft-tissue preservation. Clin Orthop Relat Res 238:249–281
4. Simpson AH, Kenwright J (2000) Fracture after distraction osteogenesis. J Bone Joint Surg Br 82(5):659–665
5. Carvalho RS, Einhorn TA, Lehmann W, Edgar C, Al-Yamani A, Apazidis A, Pacicca D, Clemens TL, Gerstenfeld LC (2004) The role of angiogenesis in a murine tibial model of distraction osteogenesis. Bone 34(5):849–861. doi:10.1016/j.bone.2003.12.027
6. Colnot C, Thompson Z, Miclau T, Werb Z, Helms JA (2003) Altered fracture repair in the absence of MMP9. Development 130(17):4123–4133
7. Lee DY, Cho TJ, Lee HR, Park MS, Yoo WJ, Chung CY, Choi IH (2010) Distraction osteogenesis induces endothelial progenitor cell mobilization without inflammatory response in man. Bone 46(3):673–679. doi:10.1016/j.bone.2009.10.018
8. Fujio M, Yamamoto A, Ando Y, Shohara R, Kinoshita K, Kaneko T, Hibi H, Ueda M (2011) Stromal cell-derived factor-1 enhances distraction osteogenesis-mediated skeletal tissue regeneration through the recruitment of endothelial precursors. Bone 49(4):693–700. doi:10.1016/j.bone.2011.06.024
9. Petit I, Jin D, Rafii S (2007) The SDF-1-CXCR4 signaling pathway: a molecular hub modulating neo-angiogenesis. Trends Immunol 28(7):299–307. doi:10.1016/j.it.2007.05.007
10. Wynn RF, Hart CA, Corradi-Perini C, O'Neill L, Evans CA, Wraith JE, Fairbairn LJ, Bellantuono I (2004) A small proportion of mesenchymal stem cells strongly expresses functionally active CXCR4 receptor capable of promoting migration to bone marrow. Blood 104(9):2643–2645. doi:10.1182/blood-2004-02-0526
11. Pead MJ, Skerry TM, Lanyon LE (1988) Direct transformation from quiescence to bone formation in the adult periosteum following a single brief period of bone loading. J Bone Miner Res 3(6):647–656. doi:10.1002/jbmr.5650030610
12. Hosogane N, Huang Z, Rawlins BA, Liu X, Boachie-Adjei O, Boskey AL, Zhu W (2010) Stromal derived factor-1 regulates bone morphogenetic protein 2-induced osteogenic differentiation of primary mesenchymal stem cells. Int J Biochem Cell Biol 42(7):1132–1141. doi:10.1016/j.biocel.2010.03.020
13. De Falco E, Porcelli D, Torella AR, Straino S, Iachininoto MG, Orlandi A, Truffa S, Biglioli P, Napolitano M, Capogrossi MC, Pesce M (2004) SDF-1 involvement in endothelial phenotype and ischemia-induced recruitment of bone marrow progenitor cells. Blood 104(12):3472–3482. doi:10.1182/blood-2003-12-4423
14. Wright LM, Maloney W, Yu X, Kindle L, Collin-Osdoby P, Osdoby P (2005) Stromal cell-derived factor-1 binding to its chemokine receptor CXCR4 on precursor cells promotes the chemotactic recruitment, development and survival of human osteoclasts. Bone 36(5):840–853. doi:10.1016/j.bone.2005.01.021
15. Askari AT, Unzek S, Popovic ZB, Goldman CK, Forudi F, Kiedrowski M, Rovner A, Ellis SG, Thomas JD, DiCorleto PE, Topol EJ, Penn MS (2003) Effect of stromal-cell-derived

factor 1 on stem-cell homing and tissue regeneration in ischaemic cardiomyopathy. Lancet 362(9385):697–703. doi:10.1016/S0140-6736(03)14232-8
16. Abbott JD, Huang Y, Liu D, Hickey R, Krause DS, Giordano FJ (2004) Stromal cell-derived factor-1alpha plays a critical role in stem cell recruitment to the heart after myocardial infarction but is not sufficient to induce homing in the absence of injury. Circulation 110(21):3300–3305. doi:10.1161/01.CIR.0000147780.30124.CF
17. Toupadakis CA, Wong A, Genetos DC, Chung DJ, Murugesh D, Anderson MJ, Loots GG, Christiansen BA, Kapatkin AS, Yellowley CE (2012) Long-term administration of AMD3100, an antagonist of SDF-1/CXCR4 signaling, alters fracture repair. J Orthop Res 30(11):1853–1859. doi:10.1002/jor.22145
18. Hatse S, Princen K, Bridger G, De Clercq E, Schols D (2002) Chemokine receptor inhibition by AMD3100 is strictly confined to CXCR4. FEBS Lett 527(1–3):255–262
19. Xu J, Wu T, Sun Y, Wang B, Zhang J, Lee WY, Chai Y, Li G (2016) Staphylococcal enterotoxin C2 expedites bone consolidation in distraction osteogenesis. J Orthop Res. doi:10.1002/jor.23372
20. Liu C, Weng Y, Yuan T, Zhang H, Bai H, Li B, Yang D, Zhang R, He F, Yan S, Zhan X, Shi Q (2013) CXCL12/CXCR4 signal axis plays an important role in mediating bone morphogenetic protein 9-induced osteogenic differentiation of mesenchymal stem cells. Int J Med Sci 10(9):1181–1192. doi:10.7150/ijms.6657
21. Xu J, Wang B, Sun Y, Wu T, Liu Y, Zhang J, Lee WY, Pan X, Chai Y, Li G (2016) Human fetal mesenchymal stem cell secretome enhances bone consolidation in distraction osteogenesis. Stem Cell Res Ther 7(1):134. doi:10.1186/s13287-016-0392-2
22. Hong P, Boyd D, Beyea SD, Bezuhly M (2013) Enhancement of bone consolidation in mandibular distraction osteogenesis: a contemporary review of experimental studies involving adjuvant therapies. J Plast Reconstr Aesthet Surg 66(7):883–895. doi:10.1016/j.bjps.2013.03.030
23. Davidson EH, Sultan SM, Butala P, Tutela JP, Canizares O, Wagner IJ, Knobel D, Saadeh PB, Warren SM (2011) Augmenting neovascularization accelerates distraction osteogenesis. Plast Reconstr Surg 128(2):406–414. doi:10.1097/PRS.0b013e31821e6e2e
24. Ceradini DJ, Kulkarni AR, Callaghan MJ, Tepper OM, Bastidas N, Kleinman ME, Capla JM, Galiano RD, Levine JP, Gurtner GC (2004) Progenitor cell trafficking is regulated by hypoxic gradients through HIF-1 induction of SDF-1. Nat Med 10(8):858–864. doi:10.1038/nm1075
25. Pacicca DM, Patel N, Lee C, Salisbury K, Lehmann W, Carvalho R, Gerstenfeld LC, Einhorn TA (2003) Expression of angiogenic factors during distraction osteogenesis. Bone 33(6):889–898
26. Li G, Simpson AH, Kenwright J, Triffitt JT (1999) Effect of lengthening rate on angiogenesis during distraction osteogenesis. J Orthop Res 17(3):362–367. doi:10.1002/jor.1100170310
27. Wang XX, Allen RJ Jr, Tutela JP, Sailon A, Allori AC, Davidson EH, Paek GK, Saadeh PB, McCarthy JG, Warren SM (2011) Progenitor cell mobilization enhances bone healing by means of improved neovascularization and osteogenesis. Plast Reconstr Surg 128(2):395–405. doi:10.1097/PRS.0b013e31821e6e10
28. Kitaori T, Ito H, Schwarz EM, Tsutsumi R, Yoshitomi H, Oishi S, Nakano M, Fujii N, Nagasawa T, Nakamura T (2009) Stromal cell-derived factor 1/CXCR4 signaling is critical for the recruitment of mesenchymal stem cells to the fracture site during skeletal repair in a mouse model. Arthritis Rheum 60(3):813–823. doi:10.1002/art.24330
29. Leucht P, Temiyasathit S, Russell A, Arguello JF, Jacobs CR, Helms JA, Castillo AB (2013) CXCR4 antagonism attenuates load-induced periosteal bone formation in mice. J Orthop Res 31(11):1828–1838. doi:10.1002/jor.22440
30. Granero-Molto F, Weis JA, Miga MI, Landis B, Myers TJ, O'Rear L, Longobardi L, Jansen ED, Mortlock DP, Spagnoli A (2009) Regenerative effects of transplanted mesenchymal stem cells in fracture healing. Stem Cells 27(8):1887–1898. doi:10.1002/stem.103
31. Luan J, Cui Y, Zhang Y, Zhou X, Zhang G, Han J (2012) Effect of CXCR4 inhibitor AMD3100 on alkaline phosphatase activity and mineralization in osteoblastic MC3T3-E1 cells. Biosci Trends 6(2):63–69